dimensional parameter extracted from the diffraction peaks is the full width at half of the maximum peak height (FWHM). It is evident from Figures 41 and 42 that there is no significant difference in FWHM, which indicates that the crystallite size of the mordenite had not changed significantly due to the catalytic testing. Absolute values have not yet been obtained for the crystallite sizes because of the uncertainty in the instrumental contribution to the linewidth.

Figures 43 and 44 show the XRD patterns of H-ZSM-5 zeolite before and after carrying out the catalytic alcohol coupling testing, respectively. The main diffraction peaks have been assigned according to data presented by Breck (34). The peaks were present in the same positions in both diffraction patterns, and there was no significant differences in the measured FWHM values. The intensity of the XRD pattern for the used H-ZSM-5 zeolite catalyst (Figure 44) was lower than for the fresh sample (Figure 43), again as expected if the used sample had some adsorbed amorphous material on the surface of the particles. These data indicate that profound changes in the zeolite structure had not occurred in terms of particle size or crystallinity due to the catalytic testing at elevated temperatures.

F. Scanning Electron Microscopy of H-Mordenite and H-ZSM-5 Zeolite

Objective

The objective of these analyses was to obtain information in regard to the sample morphology of the zeolite particles before and after the alcohol coupling reaction was carried out in the reactor system.

Experimental

Portions of the same catalysts that were utilized for the XRD analyses were used for

Figure 43. XRD pattern of H-ZSM-5 zeolite prior to catalytic testing.

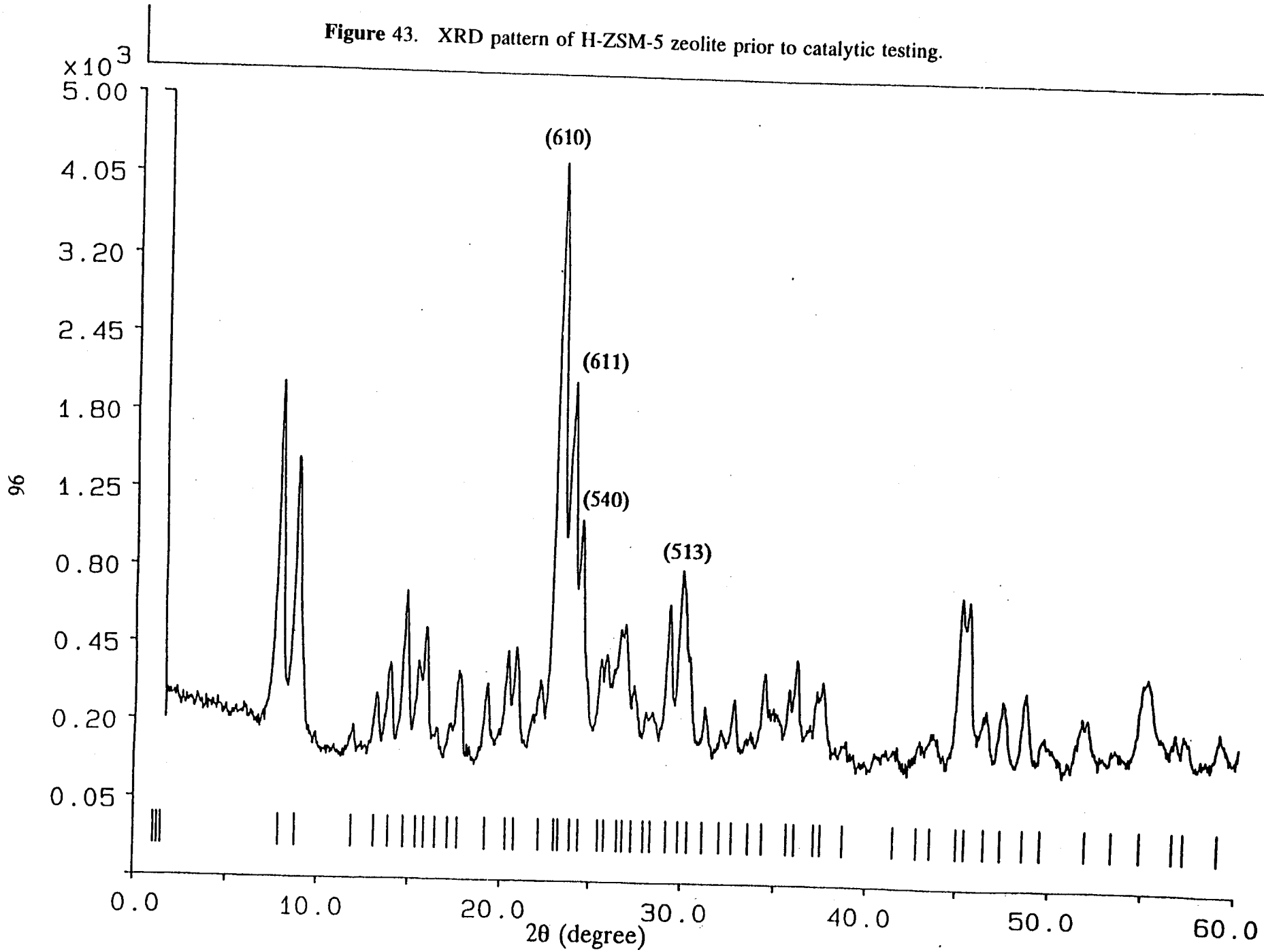

Figure 44. XRD pattern of H-ZSM-5 zeolite after catalytic testing.

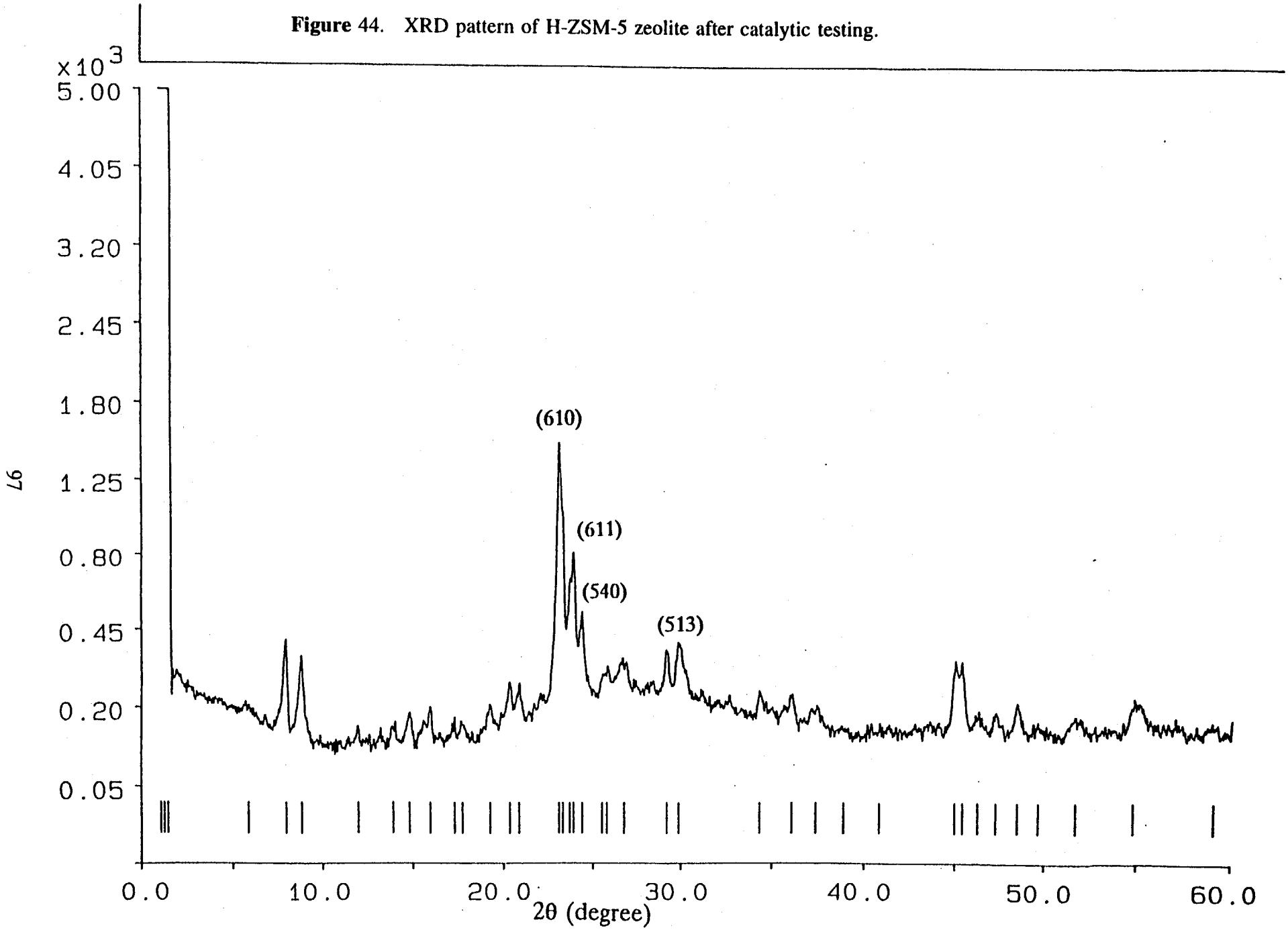

these microscopy studies. The instrument used was a Jeol JSM-6300F Scanning Microscope equipped with a field emission source. The vacuum in the sample chamber was kept at about $4 \cdot 10^{-7}$ torr.

Results

Figures 45a and 45b show electron micrographs of the H-mordenite catalyst before and after catalytic testing, respectively. It can be seen that there are small particles (≤ 1 μm), as well as larger agglomerates forming oval shaped beads. The catalytic testing at temperatures up to 150°C does not appear to have altered the particle size nor the distribution.

Figures 46a and 46b show the electron micrographs obtained with the H-ZSM-5 zeolite catalyst before and after reaction, respectively. The H-ZSM-5 zeolite exhibited a rather narrow particle size distribution compared to the H-mordenite catalyst. The catalytic testing at temperatures up to 175°C does not appear to have an effect on the H-ZSM-5 zeolite catalyst in terms of particle size or particle size distribution.

Figure 45a. Scanning electron micrograph of H-mordenite prior to catalytic testing. The magnification is 1,000 X and 10 mm equals 10 μm.

Figure 45b. Scanning electron micrograph of H-mordenite after catalytic testing. The magnification is 1,000 X and 10 mm equals 10 μm.

Figure 46a. Scanning electron micrograph of H-ZSM-5 zeolite prior to catalytic testing. The magnification is 1,000 X and 10 mm equals 10 μm.

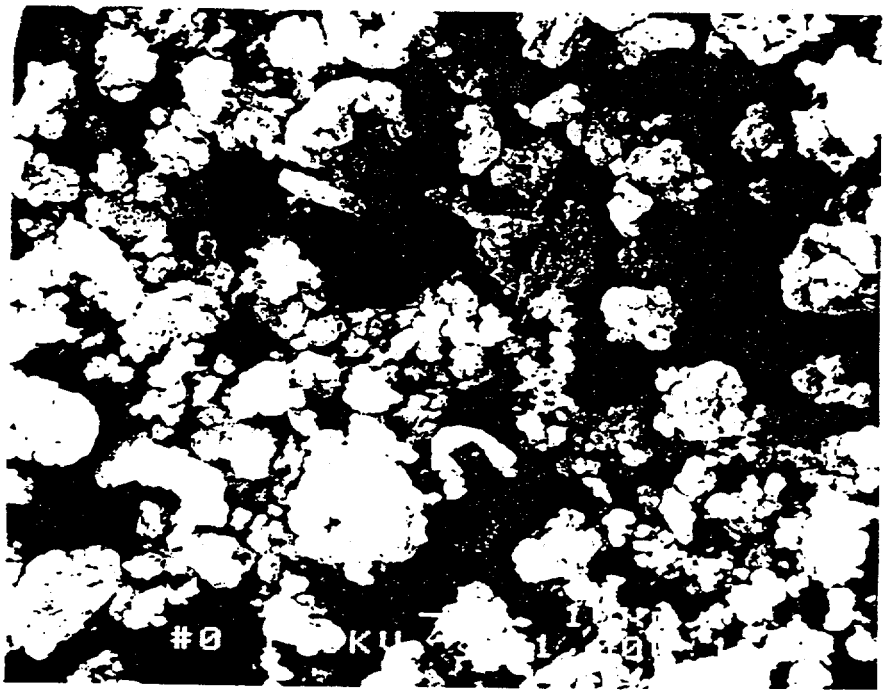

Figure 46b. Scanning electron micrograph of H-ZSM-5 zeolite after catalytic testing. The magnification is 1,000 X and 10 mm equals 10 μm.

G. Molecular Modelling of Alcohol Reactions in H-Mordenite

It has been shown in this report, e.g. see Tables 15 and 17, that mordenite, unique with respect to all other catalysts studied during this research project, was able to exclusively dehydrate methanol to dimethylether (DME), while leaving the isobutanol in the methanol/isobutanol = 1/1 reactant mixture unconverted at all but the highest temperature studied. At 150°C, 96.5% of the methanol was converted to dimethylether, while only 4.4% of the isobutanol was converted to butenes and dibutylethers.

The selective synthesis of DME was unexpected because H-mordenite is considered to be a large pore zeolite with channels of about 7 Å, while H-ZSM-5 is a medium pore zeolite with pores about 5.5 Å in diameter. The H-ZSM-5 zeolite, however, was found to be nonselective in this reaction and converted both methanol and isobutanol to many products at all temperatures studied, shown in Table 17. The extreme selectivity of H-mordenite in the reaction of the methanol/isobutanol mixture has been explored further *via* molecular modelling.

Table 17. Space Time Yields of the Products (mol/kg cat/hr) Formed Over H-Mordenite and H-ZSM-5 Zeolite from Methanol = Isobutanol = 1.72 mol/kg cat/hr Reactants in He/N_2 Carrier Gas at 0.1 MPa as a Function of Temperature.

	$T_{Reaction}$	DME	Butenes	MIBE	MTBE	C8 Ethers
H-Mordenite	90°C	0.060	------	------	------	------
	125°C	0.660	------	------	------	------
	150°C	0.830	0.068	------	------	0.004
H-ZSM-5 Zeolite	90°C	0.005	0.001	0.012	------	------
	125°C	0.071	0.169	0.350	0.004	0.003
	150°C	0.261	0.339	0.134	0.003	0.003
	175°C	0.185	1.086	0.131	0.005	0.002

H-ZSM-5 is a medium pore zeolite with interconnecting channels of the dimensions

5.3 × 5.6 Å and 5.1 × 5.5 Å. H-Mordenite is also a porous zeolite and has elliptical 7.0 x 6.5 Å channels (12-rings with openings crystallographical running in the c-direction). However, mordenite also has a system of small channels running perpendicular to the large channels (and running in the b-direction). These small channels are sometime said to consist of 3.7 x 4.8 Å channels because they have entrances of 8-ring openings (windows) of these dimensions. However, because of the mordenite structure, about 8 Å into each small pore there is a zig-zag Y-branching of the pore structure due to twisted 8-rings. This results in a distorted window to each side of the Y-branching of some 2.6 x 5.7 Å. This is a considerable restriction in the free diameter of the small channel pores through which reactant molecules can move, i.e. be transported to reactive sites in the small pores with subsequent diffusion of product molecules out of the small pores and the zeolite. The net result is that the mordenite structure is more realistically viewed as large channels having two rows of side *pockets*.

The main channels in H-mordenite are large and are accessible to isobutanol, which has a van der Waals diameter along the line joining the two methyl groups of 4.9 Å. The smaller interconnecting channel system of ZSM-5 zeolite is also accessible to isobutanol, but this oxygenate molecule is excluded from the smaller channel system of mordenite. Methanol, with a van der Waals diameter of 3.8 Å for the methyl group, has access to all channels to which isobutanol is accessible, as well as to the side pockets of mordenite.

Of interest here is the distribution of the active, strongly acidic protons in the H-mordenite. Using crystallography as a guide, it was found that the alkali ions (8 cations/unit cell) in dehydrated Na-mordenite (33) and Cs-mordenite (46) were the following: 1.5-2 in the large channels (designated as Type I), 2-3 in the 8-ring window openings to the small channel system (designated as Type II), and 3-4 inside the small channels (designated as

Types III). A ^{133}Cs NMR investigation located the Cs^+ ions at locations that were consistent with this crystallography (47). It may be assumed that the proton distribution in dry H-mordenite will be similar to those of the alkali cations, except for a shift of the protons to proximal oxygens to form OH species. The small channel protons can be located in the pocket pores on the side of the channels.

As pointed out previously, these pockets consist of an entrance 8-ring, a second parallel 8-ring at the distance of 3.5 Å from the first, and two fused oxygen 8-rings that form the bottom of the pocket. The pocket is 3.7 x 4.8 Å wide and ca. 8 Å deep, and two offset antiparallel pocket systems are wedged into each other, resulting in the ca. 2.6 Å constriction at the bottom of each pocket, to form the backbone structure surrounding the large channels. The cations located deepest in the pocket are symmetrically placed on the two sides of the bottom center oxygen of the pocket and are shared by pockets meeting at their bottoms from opposite sides. The pocket shape in mordenite resembles that of a chalice, or cup, from which the name of organic calixarenes of similar shape is derived. As the mordenite structure is made of channels surrounded by the fused cups, it could perhaps be appropriate to characterize this structure as inorganic crystalline polycalixarene.

The observed reaction selectivity whereby no isobutanol reacts in H-mordenite below 150°C, as shown in Table 17, indicates that the Type I acid sites located in the large channels are rendered unreactive. It is proposed that this poisoning of the most exposed acid sites occurs by the formation of a very strong complex between the Type I protons and isobutanol or its decomposition products. If these strong acid protons react with isobutanol to produce irreversibly bonded esters or carbenium ions or oligomeric species, they will be inaccessible for further steady state reactions with both alcohols, and only the protons located in the side pockets, which are accessible only to methanol, will be able to function

as active catalytic centers. No coke formation was observed at the reaction temperatures employed. It appears that at 150°C, the Type I acid sites begin to be regenerated, as indicated by the appearance of isobutene and C_8 ether.

The high selectivity of H-mordenite to DME at low temperatures appears to be due to a combination of selective poisoning of the large channel Type I protons by isobutanol and a size exclusion of isobutanol in reactions catalyzed by the Type III protons located in the side pockets. The role of Type II protons depends on their location. Functionally, they will act as Type I if located in the large channels and as Type III if placed inside the small channel pockets. Computer graphics have been used to model:

a. the entrance of methanol and isobutanol into the large channels and of methanol into the small channels and pockets,

b. formation of oxonium $CH_3OH_2^{\oplus}$ by reaction of methanol with the strongly acidic Type III protons,

c. S_N2 attack on this oxonium by a second methanol molecule to form DME, and

d. the exit of the DME from the small channels of the zeolite.

The cartesian coordinates of H-mordenite were obtained from the crystallographic literature (33,46). Utilizing the symmetry elements of the Cmcm space group, a large section of the zeolite was built from a limited data set. The Spartan software program from Wavefunction Inc. running on an IBM RISC 6000-based computer was used as a visualization program into which the calculated structure of H-mordenite was entered. With this implementation, the accessibilities of methanol and isobutanol molecules to potential acidic sites in the zeolite could be determined, including all of the geometries mentioned above.

In particular, it was found that methanol molecules had access to all possible proton sites in H-mordenite, especially the preferred sites in the side-pockets, Figure 47a, while these pocket sites were inaccessible to isobutanol molecules. The preferred orientation of

isobutanol in the large main channels of the zeolite is with its longest dimension parallel to those channels. Because the access to the side pockets is in a perpendicular direction to the main channels, isobutanol would have to rotate 90° in order to react with protonated methanol protruding from the side pocket Figure 47b. The computer models have shown this particular spatial configuration of the reactant molecules to be significantly strained with respect to van der Waals radii contact between isobutanol and the channel walls. This type of shape selectivity could be classified as restricted transition state selectivity. If this steric constraint were overcome and a molecule of MIBE were formed, there exists the additional larger spatial constraint of the larger MIBE molecule reorienting to its preferred trajectory through the main channels. Due to their much smaller sizes, the reactant methanol and product DME molecules do not have these impediments to reactions involving side pocket protons. It is proposed that the steric factors that the computer graphics model illustrated are important contributors to the absence of MIBE observed in the synthesis products, as well as the general lack of reactivity of isobutanol over H-mordenite.

The self-poisoning of Type I acid sites for isobutanol reactions at temperatures below 150°C occurs even in the absence of methanol, as demonstrated by separate experiments carried out here. At temperatures above 150°C, the reaction products that are formed from isobutanol in the presence and absence of methanol are the same except for DME and MIBE that contain methyl groups originating from methanol. The conversion rates of isobutanol are slightly higher in the absence of methanol as compared with methanol present, but the difference is small enough to permit the conclusion that the poisoning of Type I acid sites in the large channels is due to isobutanol only and not to preferential adsorption or reactions of methanol. This is consistent with the greater basicity of isobutanol as compared with methanol with which it competes for acid sites (16,17).

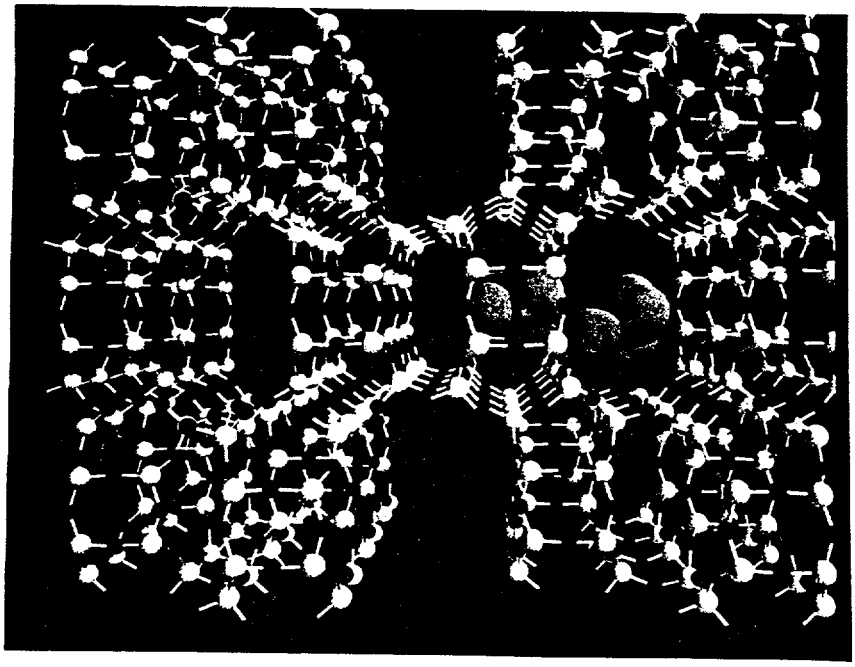

Figure 47a. Visualization of a methanol molecule in the main channel reacting with methoxonium ion in the side-pocket of H-mordenite.

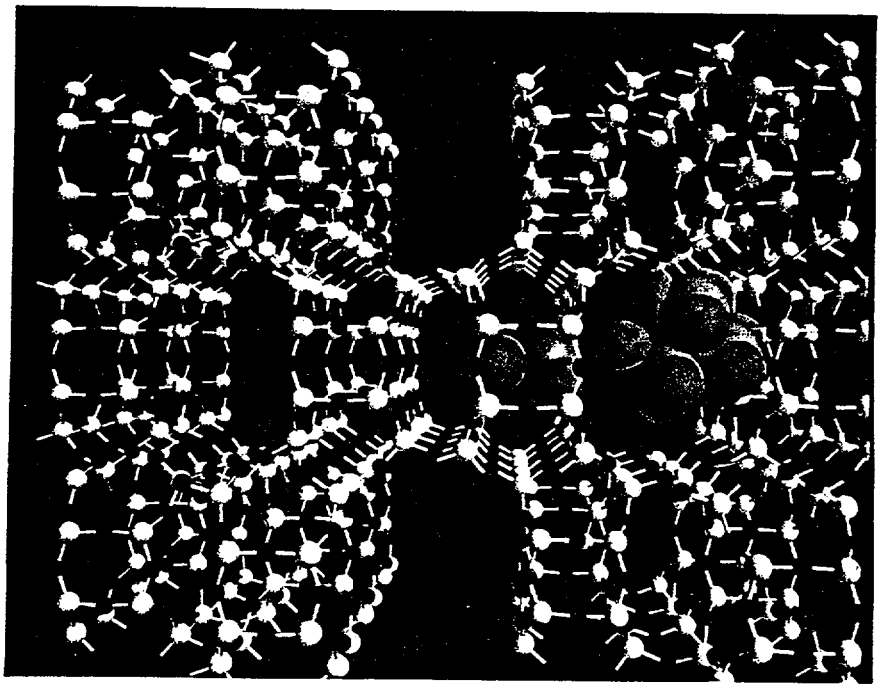

Figure 47b. Visualization of an isobutanol molecule in the main channel reacting with methoxonium ion in the side-pocket of H-mordenite. Note the size limitations of this orientation.

V. Extended Reactivity Studies Over the ZrO_2/SO_4^{2-} Catalyst

A. Alcohol Pressure Dependence on Product Selectivity

The effect of reactant pressure on the activity and selectivity of the dehydration of a 2:1 molar methanol and isobutanol mixture to butenes and ethers was studied. Nunan et al. had previously studied this reaction over Nafion-H (17). The reaction conditions chosen in the present study using ZrO_2/SO_4^{2-} as catalyst are similar to those of Nunan et al (17). To allow for kinetic analysis, the conversions were kept below 10%. The ZrO_2/SO_4^{2-} catalyst has very low activity at 116°C, and a very low space velocity was needed to induce appreciable conversion. The catalyst has high activity at 157°C and the space velocity was adjusted accordingly.

The following experimental conditions were used for the two reaction temperatures:

Temperature	116°C
Pressure (total)	0.1-7.1 MPa (1-70 atm)
Methanol feed	1.18 mol/kg catalyst/hr
Isobutanol feed	0.59 mol/kg catalyst/hr
He (+ N_2 trace) flow	20.94 mol/kg catalyst/hr
Catalyst weight	5.0 g
Temperature	157°C
Pressure (total)	0.1-6.3 MPa (1-62 atm)
Methanol feed	42.2 mol/kg catalyst/hr
Isobutanol feed	21.1 mol/kg catalyst/hr
He (+ N_2 trace) flow	756 mol/kg catalyst/hr
Catalyst weight	2.0 g

Figures 48 and 49 show the space time yields of the major products under the conditions given above as a function of total alcohol partial pressure, which was increased stepwise by sequentially increasing the reactor pressure. The results at 116°C exhibit more scatter than those at 157°C, but the trends seen are the same. It is evident that isobutene production was strongly pressure dependent, decreasing with increasing alcohol pressure. Ether production was only moderately pressure dependent, increasing somewhat with

Figure 48. Effect of alcohol partial presssure on product productivities for the reaction of methanol/isobutanol = 1/1 over the ZrO_2/SO_4^{2-} catalyst at 116°C.

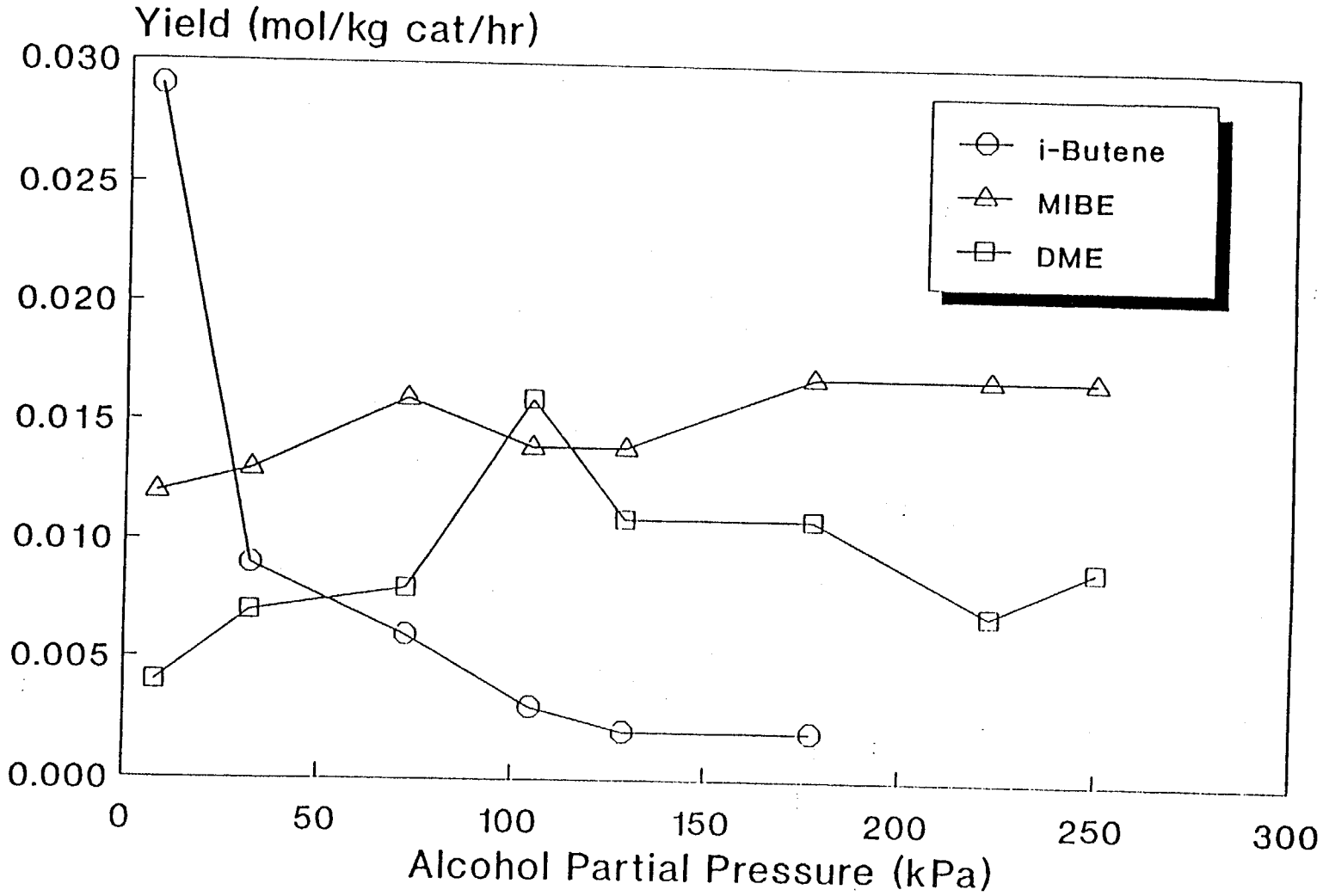

Figure 49. Effect of alcohol partial presssure on product productivities for the reaction of methanol/isobutanol = 1/1 over the ZrO_2/SO_4^{2-} catalyst at 157°C.

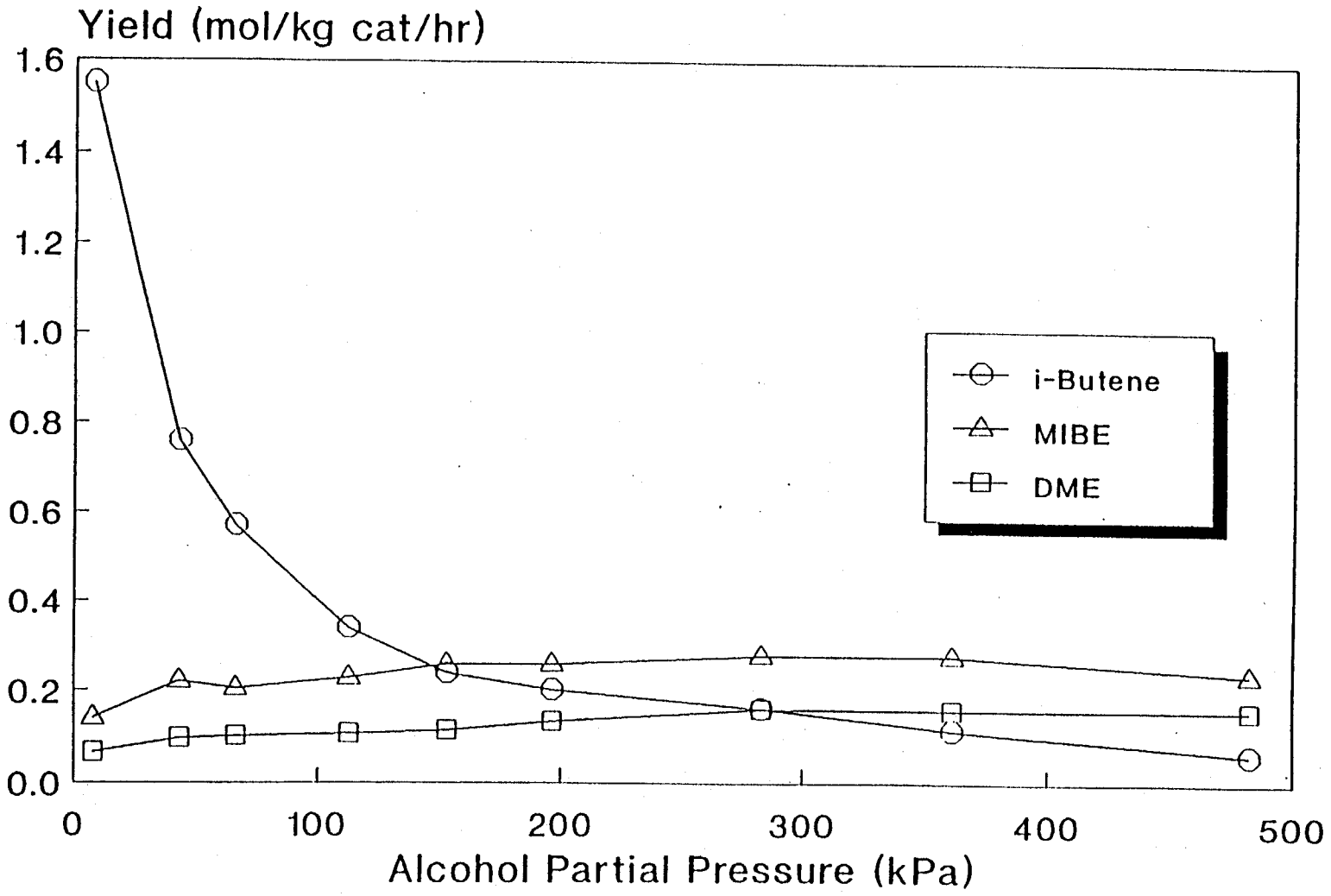

increasing alcohol pressure. Both the isobutene decrease and ether increase appear to level off to steady values. These results are similar to those observed with the Nafion-H resin catalyst (17). This suggests that the same catalytic functions and properties exist for the reaction over ZrO_2/SO_4^{2-} as was observed over Nafion-H. This pressure effect was found to be reversible in a separate experiment using fresh catalyst, i.e. when the alcohol pressure was decreased to its original value, isobutene production increased and ether production decreased to their original rates. This work also showed that the selectivity toward isobutene, which was seen previously with a 1/1 methanol/isobutanol mixture, also holds for the 2/1 methanol/isobutanol mixture used in this study at low pressures.

It is apparent from Figures 48 and 49 that low pressures are needed to maximize the selective dehydration of isobutanol to isobutene while leaving the methanol relatively unconverted. The reaction was kept far from equilibrium, and thus the effect of increasing pr essure on the reaction rate was purely a kinetic effect and not a thermodynamic one. It is also evident from Figure 50 that low temperatures are needed when pathways exist (*via* carbenium ion chemistry with Brönsted acids) for the formation of linear butenes in order to minimize the linear butenes and maximize the proportion of isobutene in the product stream. Figure 50 shows that below 150°C, i.e. the temperature range of interest, the equilibrium yield of 1-butene would be small compared to the 2-butenes.

B. Reaction of Methanol/Isobutanol Mixture over ZrO_2/SO_4^{2-} *vs* Contact Time

The kinetic studies of the methanol/isobutanol reaction over the ZrO_2/SO_4^{2-} catalyst presented above are complemented here with a study investigating the effect of contact time on the conversion and selectivity of the major reactions. The following conditions were used in these studies:

Figure 50. Equilibrium distribution of Butene isomers.

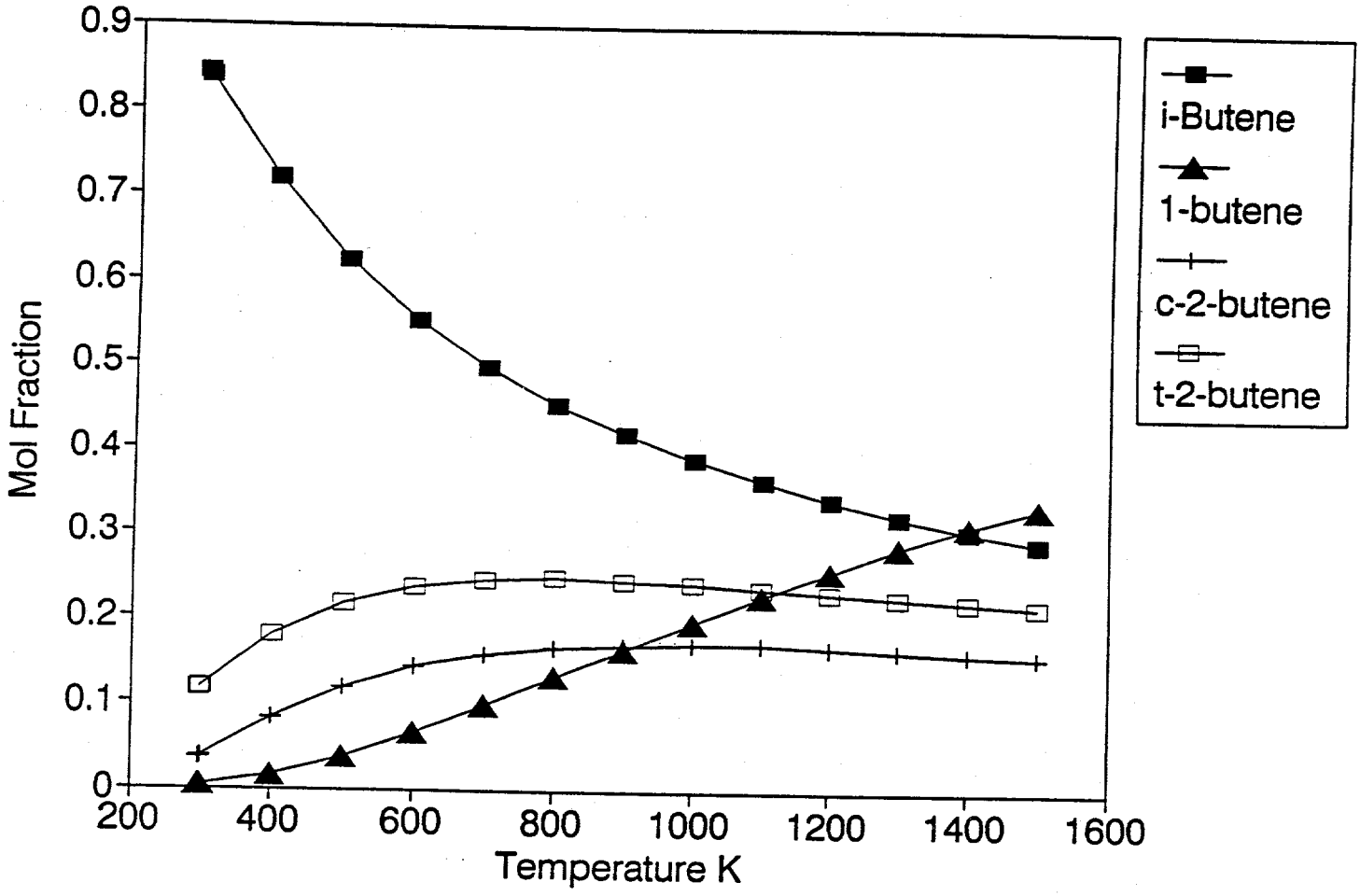

Temperature	157°C
Pressure (total)	0.1 MPa
Methanol feed	13.8-123.3 mol/kg catalyst/hr
Isobutanol feed	6.92-61.6 mol/kg catalyst/hr
He (+ N_2 trace) flow	245.2-2,207 mol/kg catalyst/hr
Zr_2/SO_4^{2-} weight	0.25 g.

The reactant mixture was a 2/1 molar MeOH/i-BuOH mixture, and the partial pressure of the alcohols was kept constant throughout the experiment by altering the space velocity of the inert gas feed (containing N_2 as an internal standard) proportionally to that of the alcohols. In the usual manner, a fresh ZrO_2/SO_4^{2-} sample calcined to 620°C was charged into the reactor, the gas flow rates were adjusted, and the reactor was brought to the reaction temperature. The experiment started with the highest space velocities, which were sequentially lowered. Product analysis at each space velocity was the average of multiple sampling at each point. The contact times were defined as 1/GHSV. The space velocity has been converted from mol reactant/(kg cat. hr) to STP liter of reactant gas/(liter catalyst × min) *via* the ideal gas equation and assuming that the volume of 1 kg catalyst = 1 liter.

Figure 51 shows the percent conversion of isobutanol *vs* the contact time. A linear relationship existed over the entire range tested, indicating that reaction studies within this range of contact times were within the kinetic regime. The kinetic data lie well within the bounds of the kinetic regime, thus establishing that kinetic interpretation of the data is valid.

The butene product selectivity as a function of contact time is presented in Figure 52. It is clear that isobutene was the predominant butene formed, and it was produced at a higher percentage, i.e. 86-88 mol%, than that calculated for thermodynamic equilibrium, ca. 70%, at the reaction temperature of 157°C, Figure 50. It is also interesting to note that the selectivity of *cis*-2-butene is now comparable to, or even greater than, that of the *trans*-2-

Figure 51. Contact time dependence of the reaction of methanol/isobutanol = 2/1 over the ZrO_2/SO_4^{2-} catalyst at 157°C.

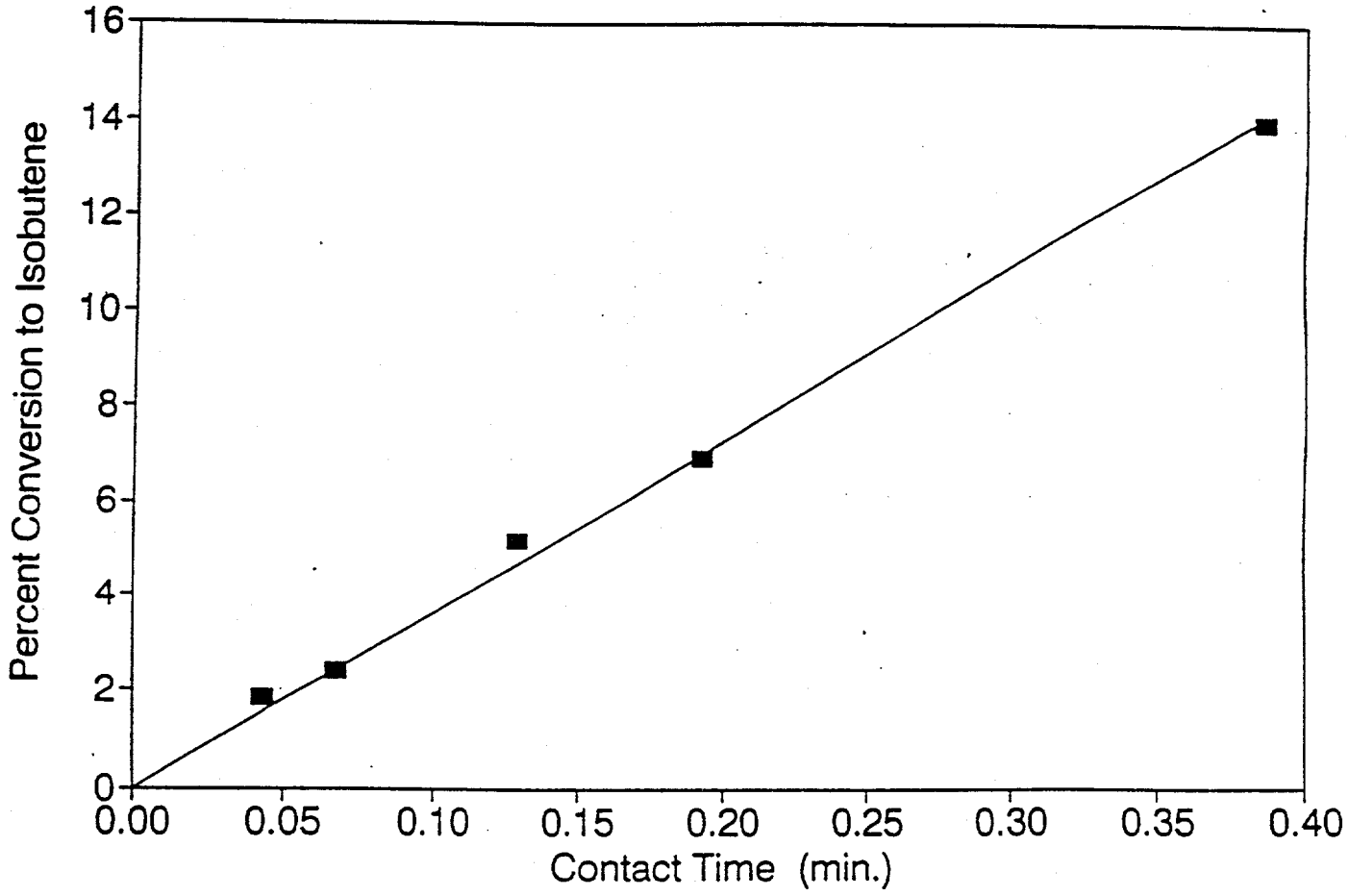

Figure 52. Butene product selectivity of the reaction of methanol/isobutanol = 2/1 over the ZrO_2/SO_4^{2-} catalyst at 157°C.

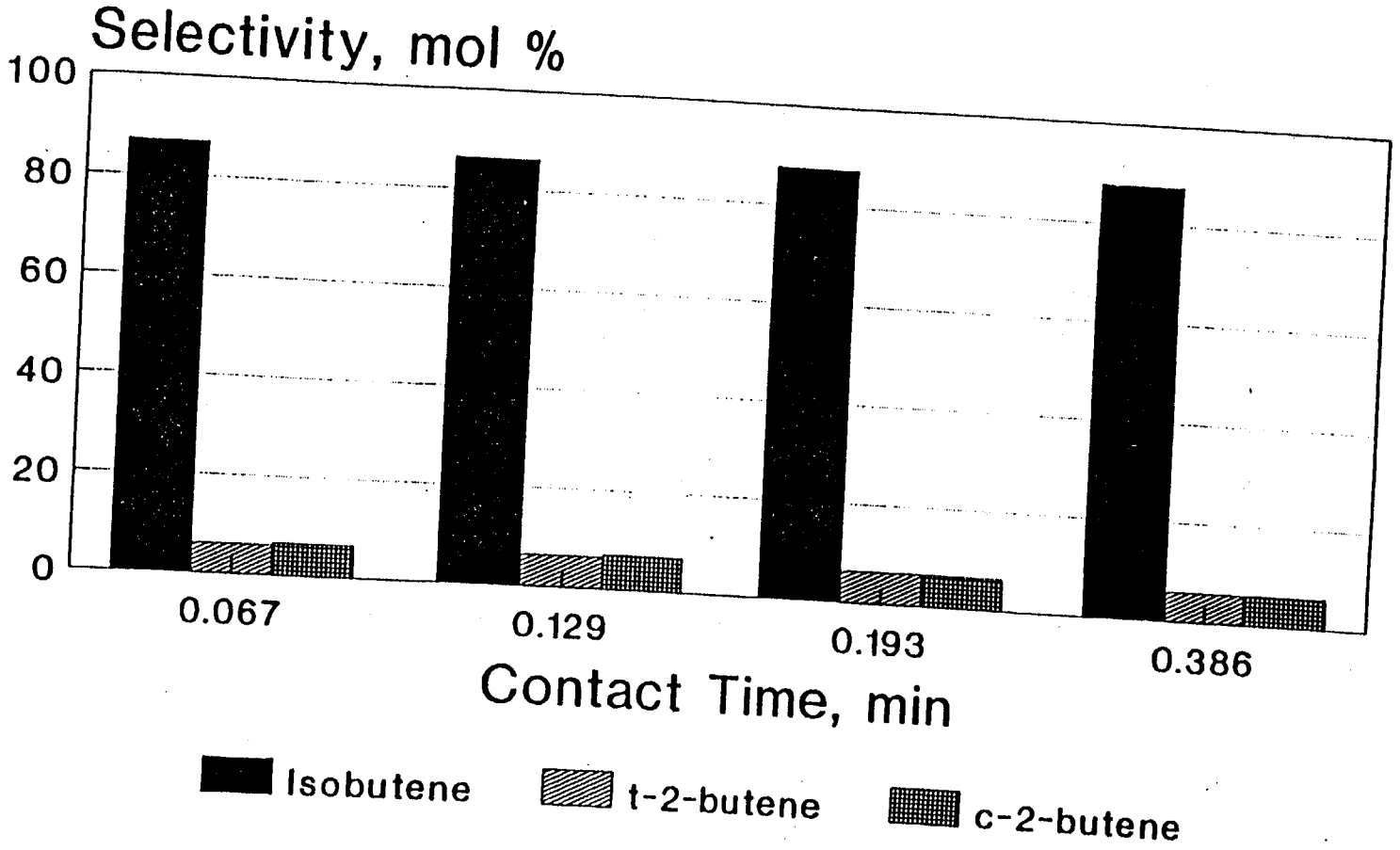

butene product, in contrast to the relative yields expected from equilibrium considerations (48). In addition, the composition of butenes with respect to selectivity remains constant over the range of contact times, and thus conversion levels of isobutanol, studied. This indicates that the linear butenes are also primary products and not the result of secondary isomerization of the isobutene produced in the reaction, in accordance with other studies (49).

C. Effect of Isobutanol Pressure on Mixed Alcohol Dehydration

The effect of increasing isobutanol pressure while maintaining the methanol partial pressure constant was investigated. Each alcohol flow was controlled with separate pumps. The following experimental conditions were used:

Temperature	157°C
Pressure (total)	0.1 MPa
Methanol feed	42.5 mol/kg catalyst/hr
Isobutanol feed	5.41-216.4 mol/kg catalyst/hr
He (+ N_2 trace) flow	778.3 mol/kg catalyst/hr
Zr_2/SO_4^{2-} weight	0.40 g

Figure 53 presents the space time yields of the major products of the mixed alcohol dehydration. As the pressure of isobutanol was increased, the production of isobutene and MIBE initially increased, but at higher isobutanol pressures they tended to decrease. DME tended to decrease consistently as the isobutanol pressure increased.

D. Pressure Dependence of Methanol Dehydration

To complete the alcohol pressure dependence study on sulfate-modified zirconia, methanol was utilized as the reactant in the absence of isobutanol. The following experimental conditions were used:

Figure 53. Space time yields of products as a function of isobutanol pressure over the ZrO_2/SO_4^{2-} catalyst at 157°C and 0.1 MPa total pressure.